

Electronic Supplementary Information

High Proton Conductivity at Low Relative Humidity in an Anionic Fe-based Metal-Organic Framework

Thach N. Tu,^a Nghi Q. Phan,^a Thanh T. Vu,^a Ha L. Nguyen,^a Kyle E. Cordova,^{a,b,*} and
Hiroyasu Furukawa^{a,b,c,*}

^aCenter for Molecular and NanoArchitecture (MANAR), Viet Nam National University,
Ho Chi Minh City, 721337 (Vietnam)

^bDepartment of Chemistry, University of California – Berkeley, Center for Global
Science at Berkeley, Berkeley, CA 94720 (USA)

^cKing Fahd University of Petroleum and Minerals, Dhahran, 34464 (Saudi Arabia)

*To whom correspondence should be addressed: furukawa@berkeley.edu,
kcordova@berkeley.edu

Table of Contents

Section S1	<i>Materials and Analytical Techniques</i>	S3-S4
Section S2	<i>Synthesis of VNU-15</i>	S5
Section S3	<i>Single Crystal X-ray Diffraction Analysis</i>	S6-S7
Section S4	<i>Powder X-ray Diffraction Patterns of VNU-15</i>	S8
Section S5:	<i>Fourier Transform Infrared Analysis (FT-IR) of Activated VNU-15</i>	S9
Section S6	<i>Thermal Gravimetric Analysis (TGA)</i>	S10
Section S7	<i>Gas and Vapor Adsorption Studies</i>	S11-S14
Section S8	<i>Proton Conductivity Studies</i>	S15-S23
Section S9	<i>Stability of VNU-15 during Proton Conductivity Studies</i>	S24-S27
Section S10	<i>References</i>	S28

Section S1: Materials and Analytical Techniques

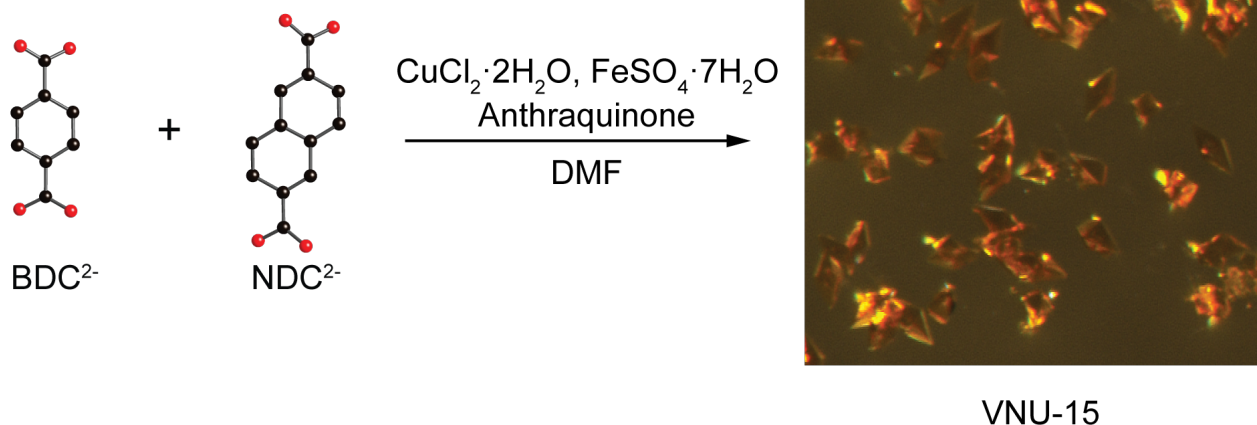
Materials. 9,10-Anthraquinone was purchased from Merck Co. Iron sulfate heptahydrate ($\text{FeSO}_4 \cdot 7\text{H}_2\text{O}$, 99% purity), copper chloride dihydrate ($\text{CuCl}_2 \cdot 2\text{H}_2\text{O}$, 99% purity), benzene-1,4-dicarboxylic acid (H_2BDC , 98% purity), and naphthalene-2,6-dicarboxylic acid (H_2NDC , 98% purity) were purchased from Sigma-Aldrich. Anhydrous *N,N*-dimethylformamide (DMF, 99% extra dry grade) and dichloromethane (DCM, 99% extra dry grade) were obtained from Sigma-Aldrich and Acros, respectively.

Analytical techniques. A single crystal of VNU-15 was mounted on a cryoloop and cooled down to 100 K by a nitrogen flow controlled by a Kryoflex II system. A Bruker D8 Venture diffractometer was used with X-rays generated by a monochromatic microfocus Cu K α radiation source ($\lambda = 1.54178 \text{ \AA}$) at 50 kV and 1.0 mA. The diffraction data was collected by a PHOTON-100 CMOS detector. The unit cell was determined using Bruker SMART APEX II software suite. The data set was reduced and data correction was carried out by a multi-scan spherical absorption method. The structure was solved by direct methods and further refinement was carried out using the full-matrix least-squares method in the SHELX-97 program package. After locating the framework backbone atoms, the SQUEEZE routine in PLATON was used to remove residual electron density from solvent molecules inside VNU-15.¹ The final structure was anisotropically refined (except C4) using modified electron density map obtained from the SQUEEZE routine. Powder X-ray diffraction (PXRD) patterns were collected using a D8 Advance diffractometer equipped with a LYNXEYE detector. Thermal gravimetric analysis (TGA) was performed using a TA Instruments Q-500 thermal gravimetric analyzer under a gas mixture of O₂ (20%) and N₂ (80%) with temperature ramp of 5 °C min⁻¹. Fourier transform infrared (FT-IR) spectra were measured on a Bruker ALPHA FTIR spectrometer using potassium bromide pellets. Low-pressure N₂ and CO₂ adsorption measurements were carried out on a Quantachrome Autosorb iQ volumetric gas adsorption analyzer. A liquid N₂ bath was used for measurements at 77 K. Helium was used as estimation of dead space. Ultrahigh-purity-grade N₂, and He (99.999% purity) were used throughout adsorption experiments. High grade CO₂ (99.95% purity) was used for the respective adsorption experiments. Water uptake of VNU-15 was

measured using a BELSORP-aqua3 with the experiment temperature being controlled via a water circulator. Elemental analysis was performed in the Microanalytical Laboratory of the College of Chemistry at UC Berkeley using a Perkin Elmer 2400 Series II combustion analyzer. The amount copper in VNU-15 was measured by atomic absorption spectroscopy (AAS) that was performed at Vietnam Academy of Science and Technology using a Shimadzu AA 6200 atomic absorption spectrophotometer. Impedance analysis of VNU-15 pelleted samples (13 mm diameter, pressed at 3 tons cm^{-2}) was carried out on a Gamry potentiostat (model Interface 1000) using the two-probe method. Humidity was controlled by an Espec humidity chamber (model SH-222). The measuring frequency ranged from 1 MHz to 10 Hz. The applied voltage varied from 1 mV to 30 mV depending on open circle voltage. The thickness of VNU-15 pallet was measured using a Nikon SMZ1000 microscope, with a typical pellet thickness ranging from 0.4 to 0.5 mm.

Section S2: Synthesis of VNU-15

A mixture of H₂BDC (60 mg, 0.36 mmol), H₂NDC (60 mg, 0.27 mmol), 9,10-anthraquinone (30 mg, 0.25 mmol), FeSO₄·7H₂O (60 mg, 0.143 mmol), and CuCl₂·2H₂O (60 mg, 0.35 mmol) was dissolved in 10 mL of DMF. The solution was sonicated for 10 min and then divided between six borosilicate glass tubes (1.7 mL each tube). The glass tubes were subsequently flame sealed under ambient atmosphere and temperature and placed in an isothermal oven, preheated at 165 °C, for four days to yield reddish-yellow crystals of VNU-15. These crystals were washed with 10 mL of DMF (6 times) and immersed in DMF three days before exchanging the solvent with 10 mL of DCM over two days (6 times for exchanging solvent). Thereafter, VNU-15 was heated at 100 °C to obtain 34 mg (0.051 mmol) of guest free VNU-15 (71.3% yield based on iron). Note: MIL-53 was formed in the absence of 9,10-anthraquinone to the reaction mixture.² Furthermore, MIL-88 was formed without CuCl₂·2H₂O added to the reaction mixture.³ EA (CHNS) of activated VNU-15: Calcd. for Fe₄C_{37.8}H_{71.4}N_{4.68}O_{38.64}S₄ = {[Fe₄(NDC)(BDC)₂(DMA)_{4.2}(SO₄)₄]·0.4DMF}·10H₂O: C, 29.38; H, 4.62; N, 4.25; S, 8.29%. Found: C, 28.95; H, 4.64; N, 4.74; S, 8.13%. AAS of activated VNU-15: 0.036 wt% of copper.



Scheme S1. Synthetic scheme for crystallizing reddish-yellow, octahedral VNU-15.

Section S3: Single Crystal X-ray Diffraction Analysis

Table S1. Crystal data and structure refinement for VNU-15

Empirical formula	$C_{18}H_{21}N_2O_{14}S_2Fe_2$
Formula weight	665.19
Temperature (K)	100
Wavelength (Å)	1.54178
Crystal system	Orthorhombic
Space group	<i>Fddd</i>
Unit cell dimensions (Å)	$a = 16.7581(7)$
	$b = 18.8268(9)$
	$c = 38.9998(18)$
Volume (Å ³)	12304.5(10)
Z	16
Density (g cm ⁻³)	1.436
Absorption coefficient (mm ⁻¹)	9.385
<i>F</i> (000)	5424
Crystal size (mm)	0.131 × 0.143 × 0.234
θ range (°)	3.6931 to 67.9142.
Index ranges	$-19 \leq h \leq 19, -21 \leq k \leq 21, -44 \leq l \leq 45$
Reflections collected	18293
Independent reflections	2535 [$R_{\text{int}} = 0.1476$]
Completeness to $\theta = 67.9142^\circ$	0.999
Data / restraints / parameters	18293 / 0 / 196
S (GOF)	1.070
R_1, wR_2 [$I > 2\sigma(I)$]	0.0547, 0.1226
R_1, wR_2 (all data)	0.0768, 0.1324
Largest diff. peak and hole (e·Å ⁻³)	0.651 and -0.401

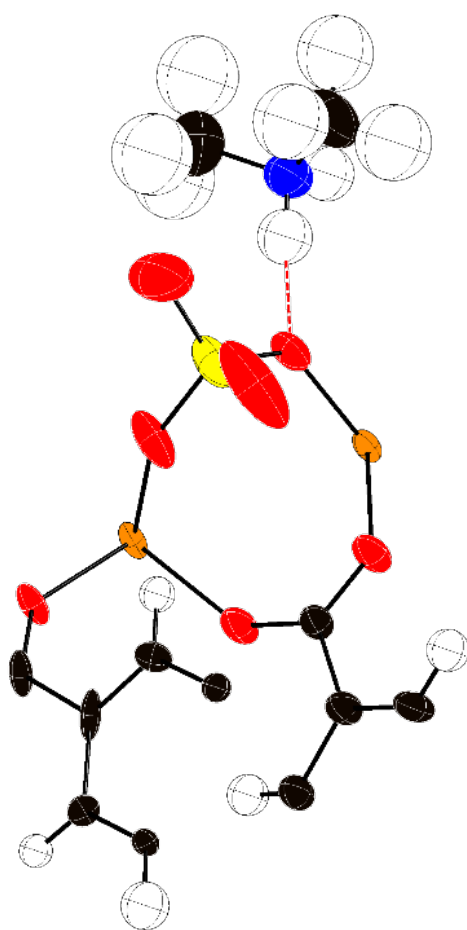


Fig. S1. Thermal ellipsoid plot of the asymmetric unit of VNU-15 with 50% probability.

Section S4: Powder X-ray Diffraction Patterns of VNU-15

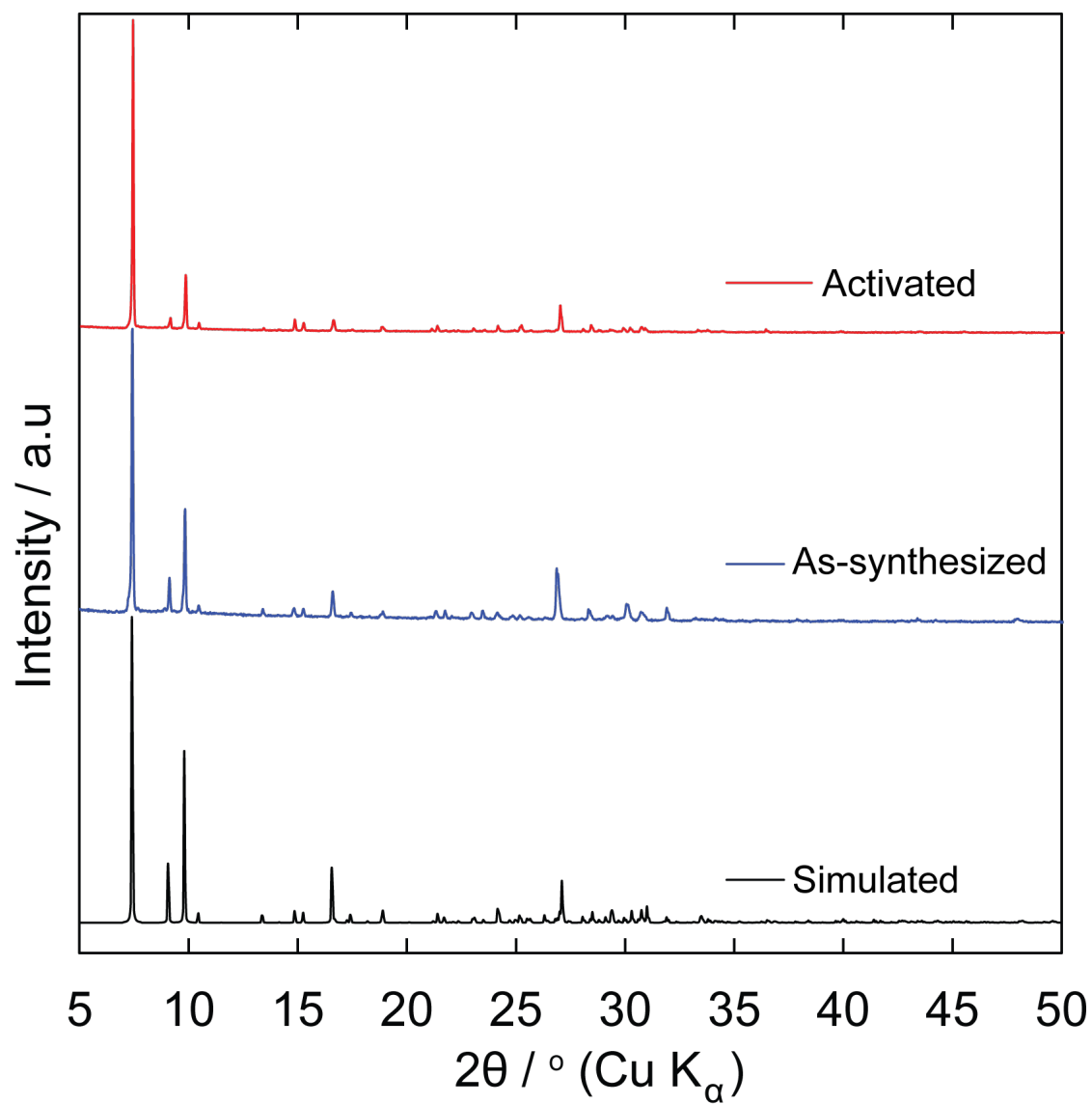


Fig. S2. The calculated PXRD pattern of VNU-15 from single crystal data (black) compared with the experimental patterns from the as-synthesized sample (blue) and samples after activation at 100 °C (red).

Section S5: Fourier Transform Infrared Analysis (FT-IR) of Activated VNU-

15

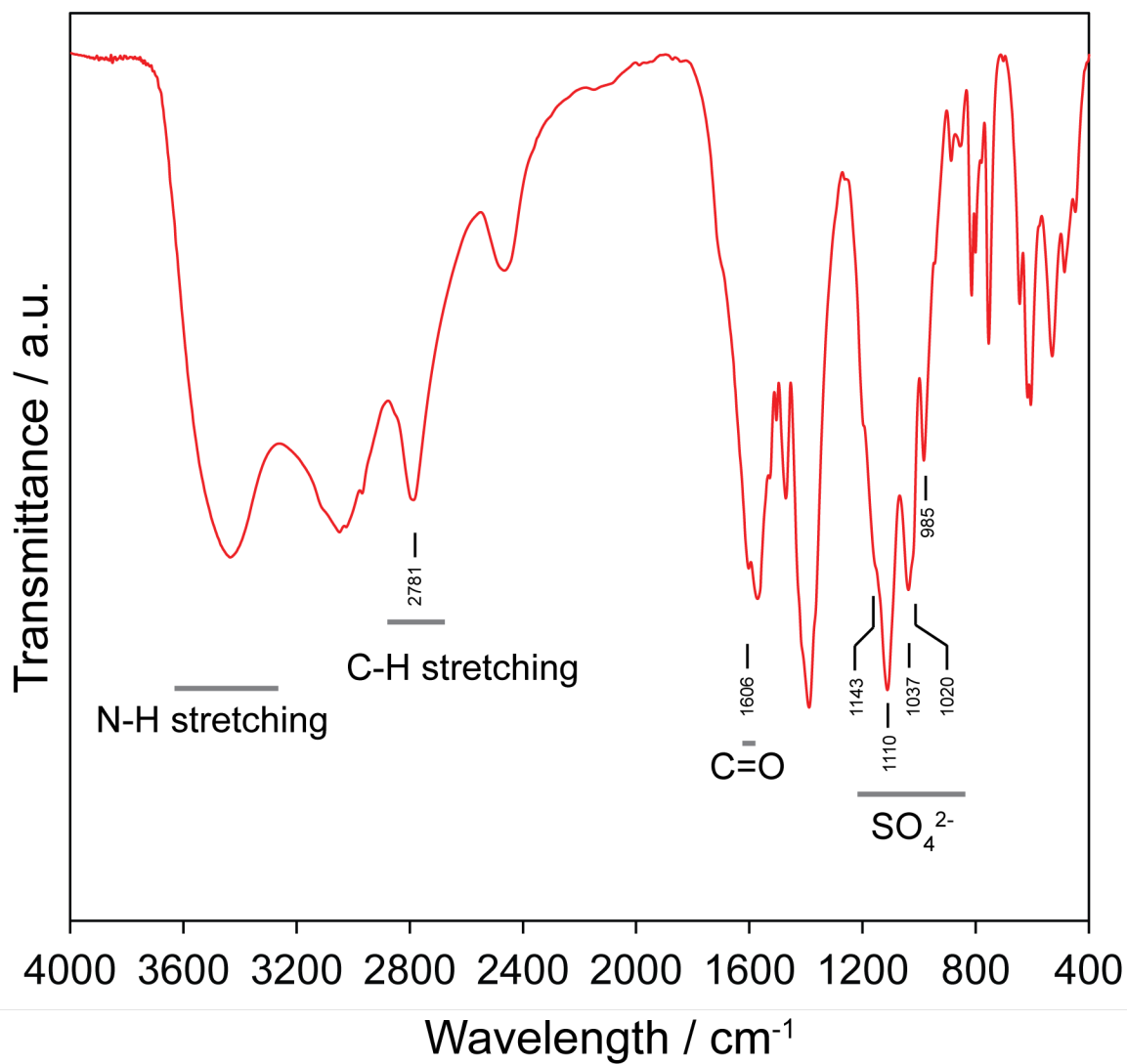


Fig. S3. FT-IR spectra of activated VNU-15.

Section S6: Thermal Gravimetric Analysis (TGA) of VNU-15

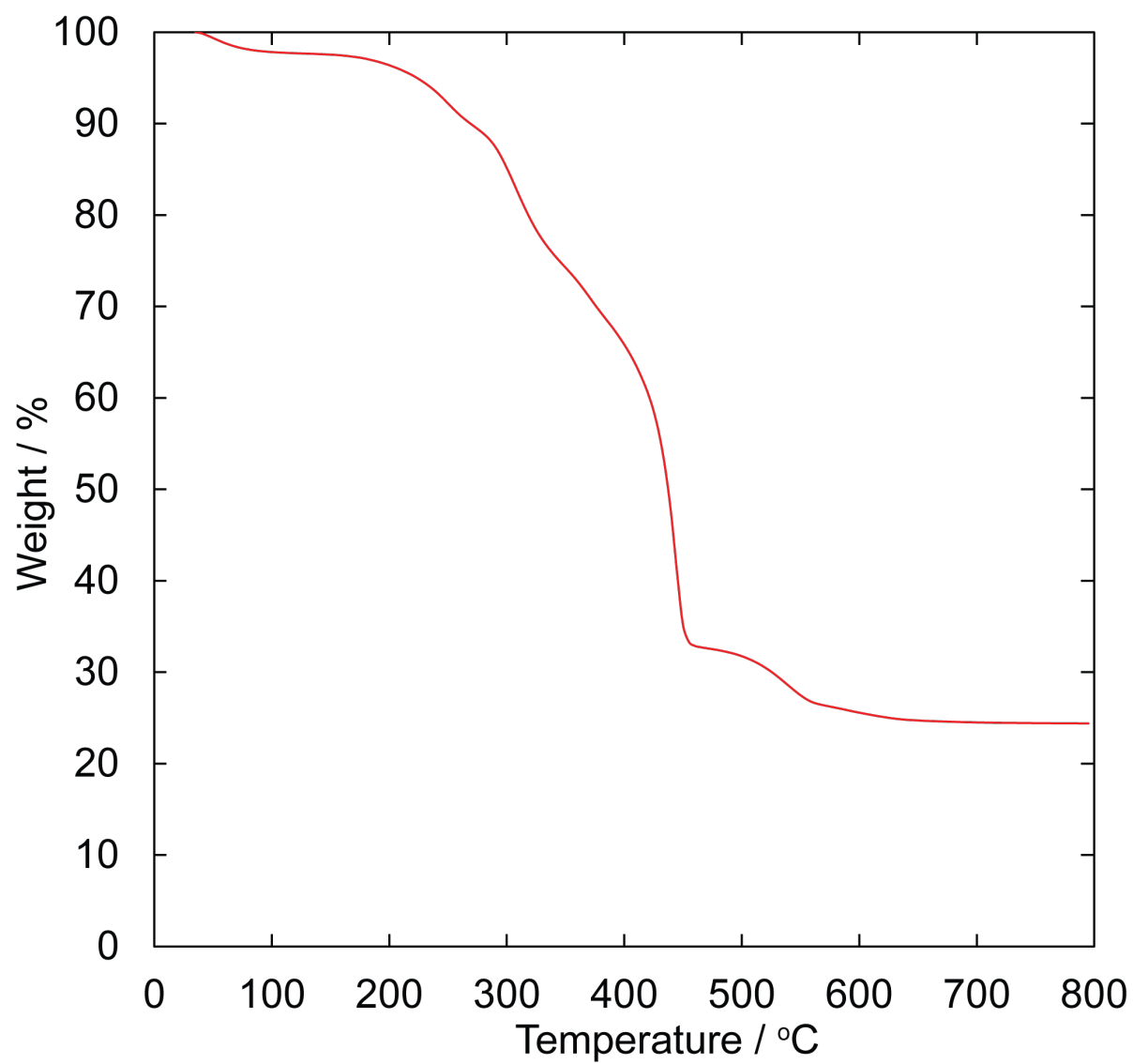


Fig. S4. TGA curves of activated VNU-15 under airflow.

Section S7: Gas and Vapor Adsorption Studies

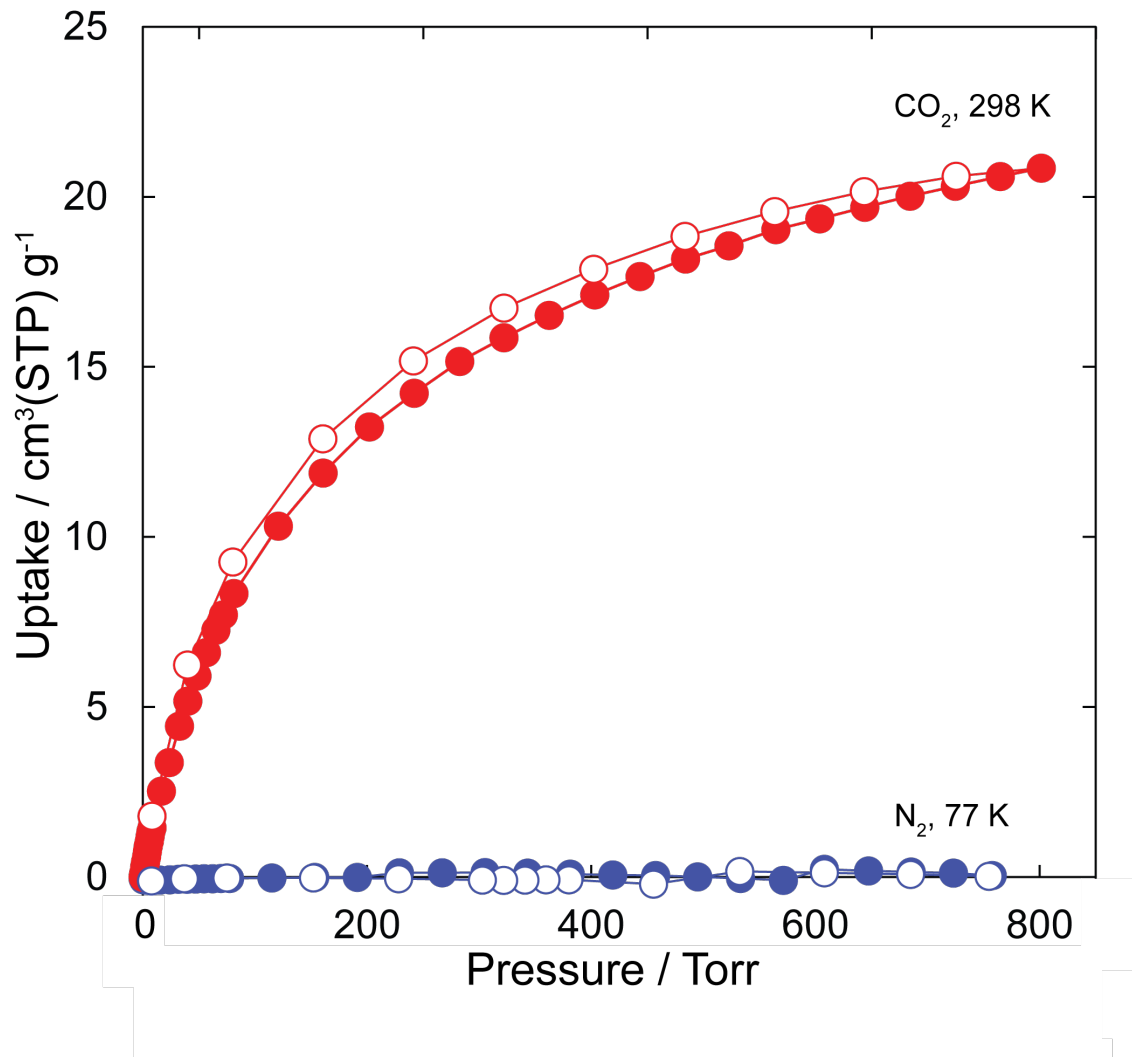


Fig. S5. N₂ (blue) and CO₂ (red) uptake of VNU-15 at 77 K and 298 K, respectively. The closed and open circles represent the adsorption and desorption branches of the isotherm, respectively. The connecting line functions as a guide for eye.

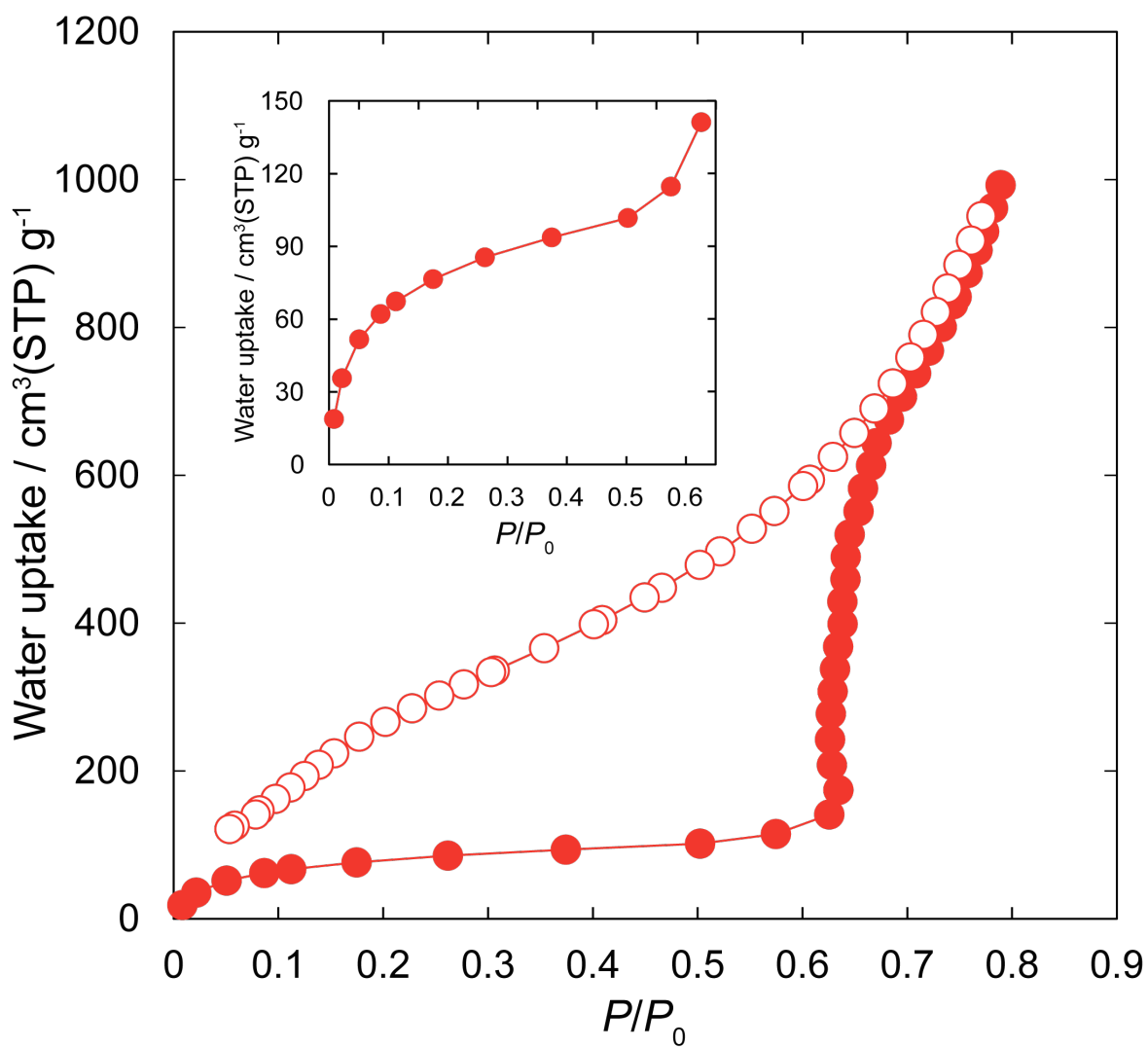


Fig. S6. Water uptake of VNU-15 at 25 °C as a function of P/P_0 ranging from 8% to 80%. Inset: Water uptake of VNU-15 at 25 °C with P/P_0 ranging from 8% to 62.58%.

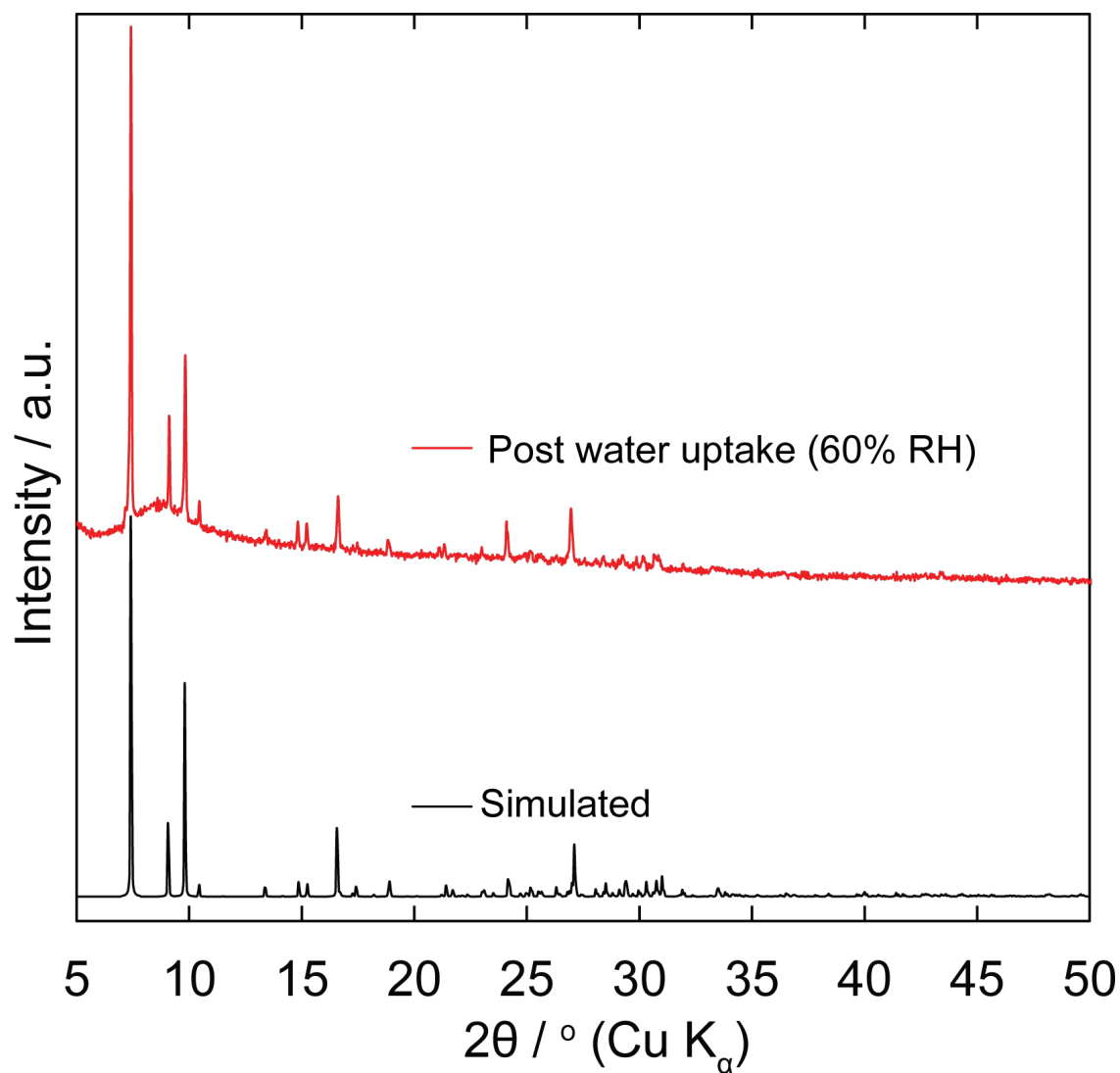


Fig. S7. PXRD analysis of VNU-15 exhibiting the long range order of the structure was retained after water uptake up to 60% RH at 25 °C. The experimental pattern (red) corresponded well with the simulated (black) diffraction pattern of VNU-15 from single crystal data.

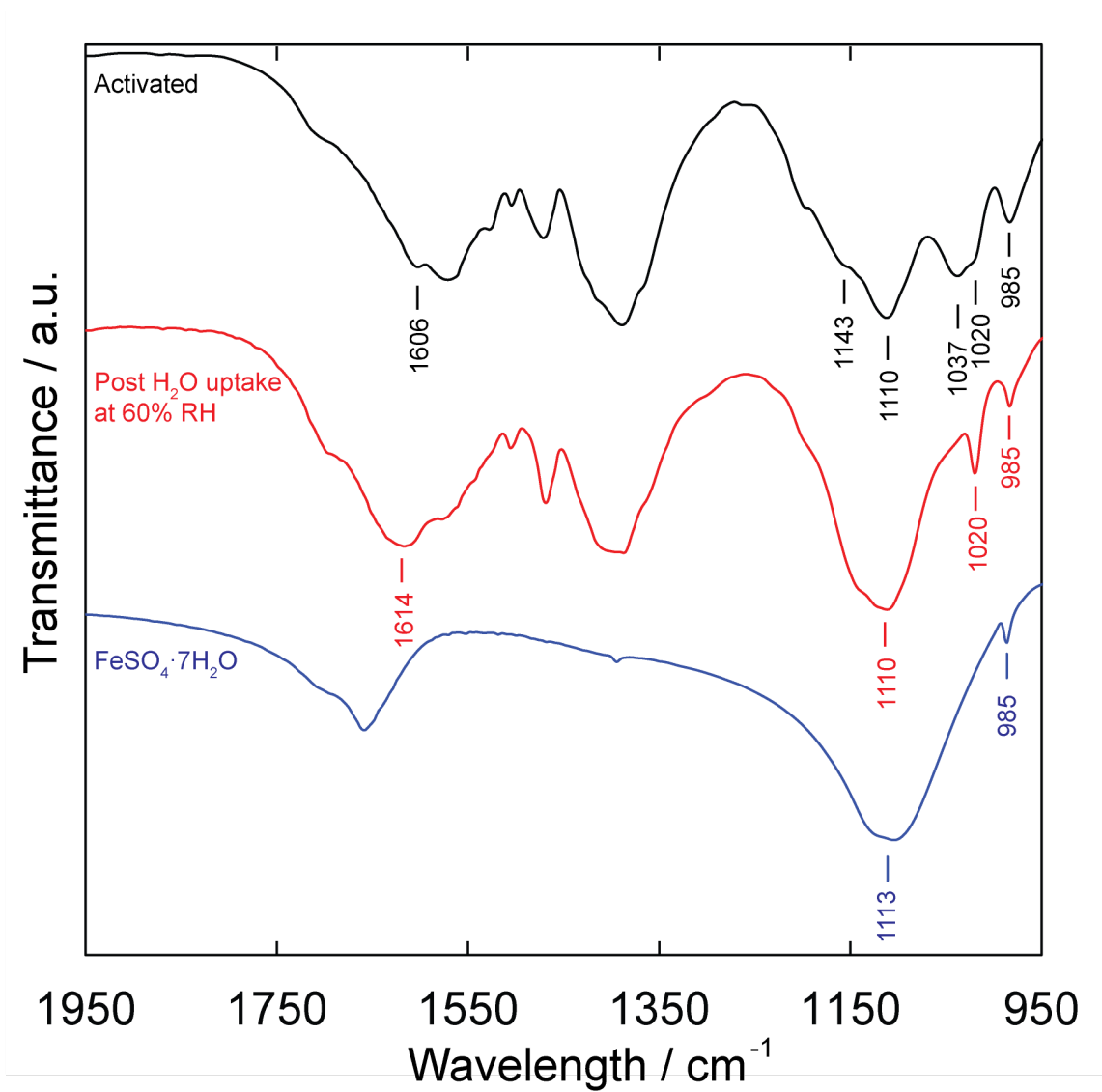


Fig. S8. FT-IR spectra of VNU-15, post H₂O uptake at 60% RH, as compared to activated VNU-15 and FeSO₄·7H₂O.

Section S8: Proton Conductivity Studies

It is noted that the impedance of the electric wire without pelleted VNU-15 was collected in order to correct for the inductive effect.⁴ The correction was carried out by subtracting the experimental impedance of pelleted VNU-15 from the experimental impedance of the electric wire in order to obtain the pure impedance of pelleted VNU-15.

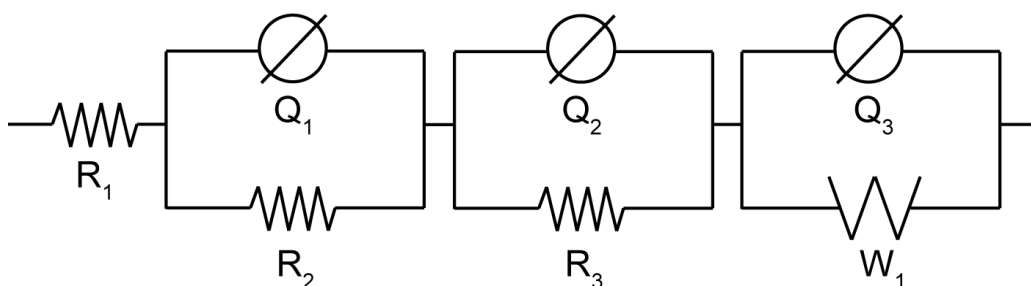


Fig. S9. An equivalent circuit used for fitting. Schematic representations: W_1 , Warburg diffusion element; $Q_1/Q_2/Q_3$, imperfect capacitor; R_1 , Contact resistor; R_2 , bulk resistor; R_3 , grain boundary resistor.

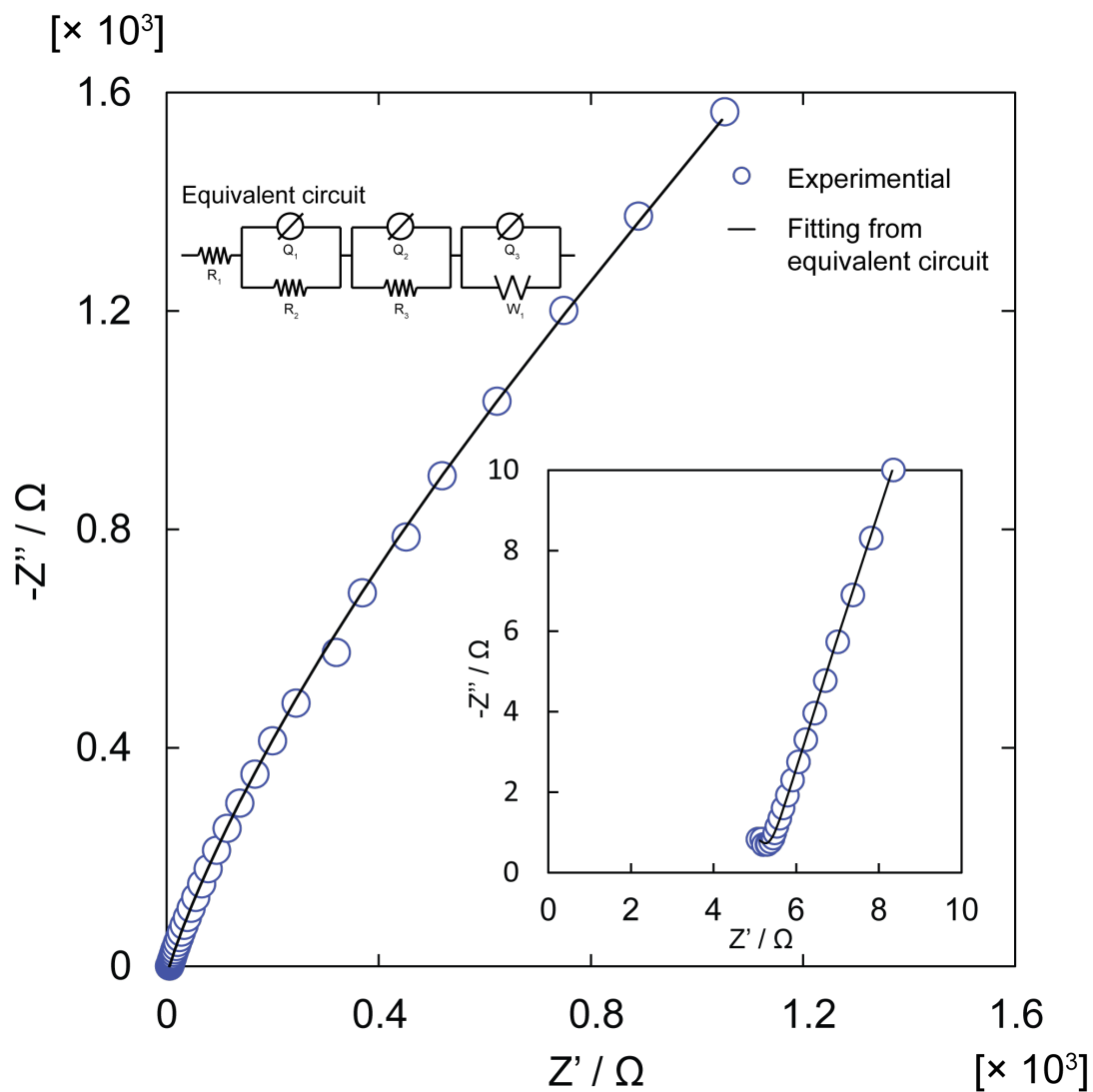


Fig. S10. Nyquist plot derived from equivalent circuit (black line) and experimental Nyquist plot (blue circles) of pelletized VNU-15 under 60% RH at 25 °C. Frequency ranged from 1 MHz to 10 Hz. Inset: Zoom of Nyquist plot at high frequency.

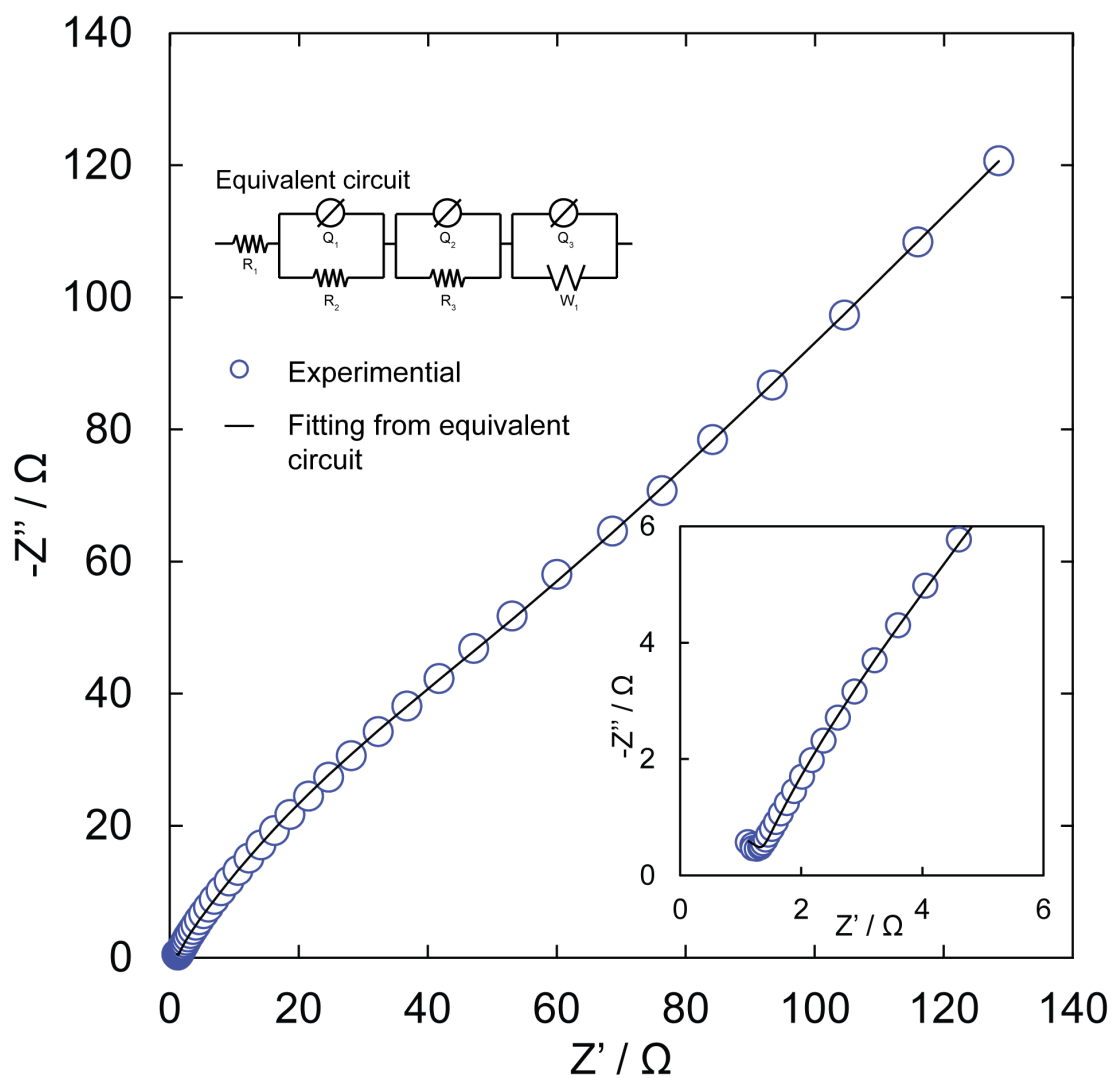


Fig. S11. Nyquist plot derived from equivalent circuit (black line) and experimental Nyquist plot (blue circles) of pelletized VNU-15 under 60% RH at 95 °C. Frequency ranged from 1 MHz to 10 Hz. Inset: Zoom of Nyquist plot at high frequency.

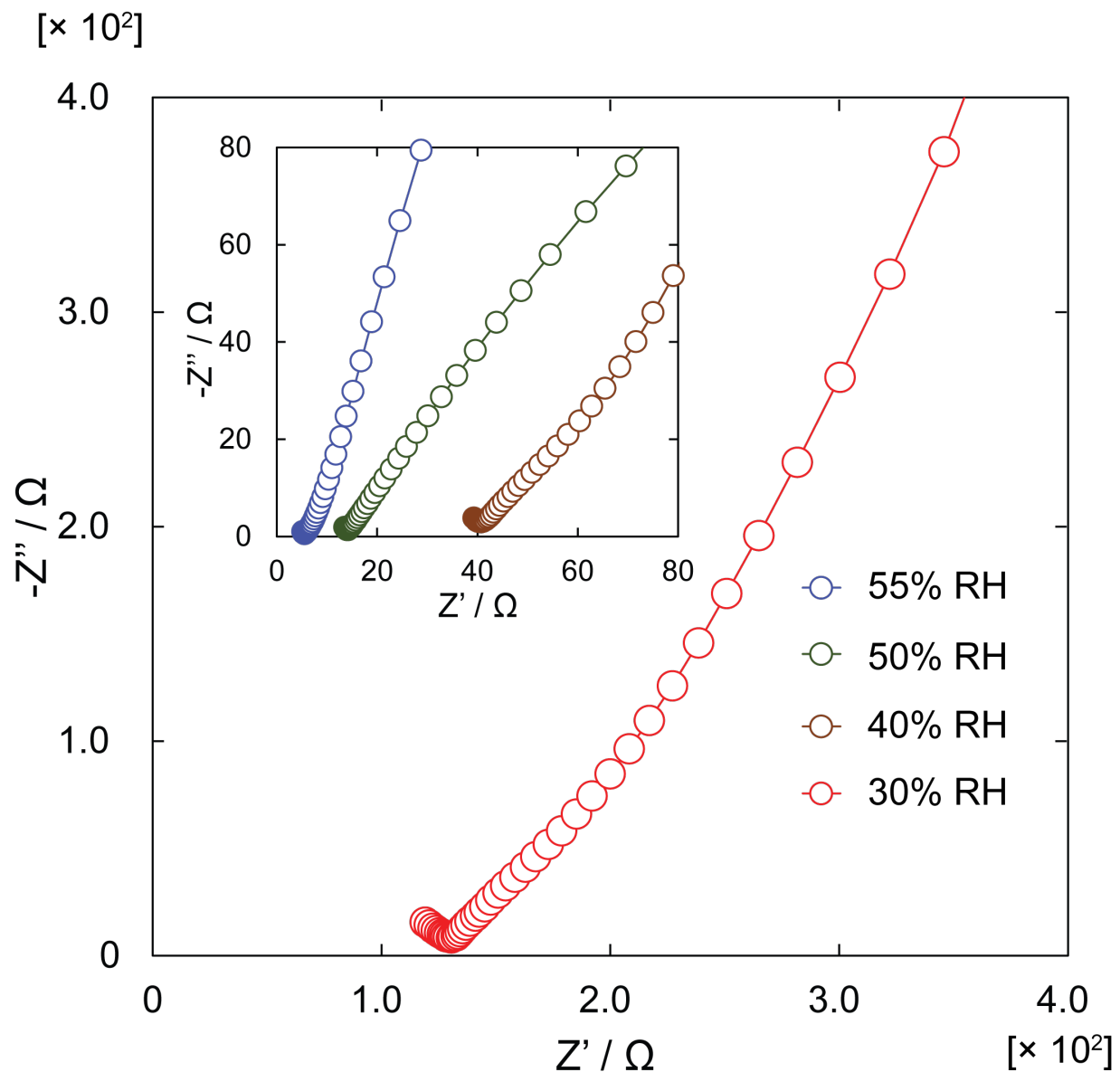


Fig. S12. Nyquist plots of pelletized VNU-15 under 30% RH at 95 °C (red circles). Inset: Nyquist plots of pelletized VNU-15 under 40% RH (brown circles), 50% RH (green circles) and 55% RH (blue circles) at 95 °C.

Table S2. Relative humidity and proton conductivity dependence of pelletized VNU-15 at 95 °C.

Temp / °C	RH / %	σ / S cm ⁻¹
95	30	2.38×10^{-4}
	40	7.77×10^{-4}
	50	2.22×10^{-3}
	55	5.77×10^{-3}
	60	2.90×10^{-2}

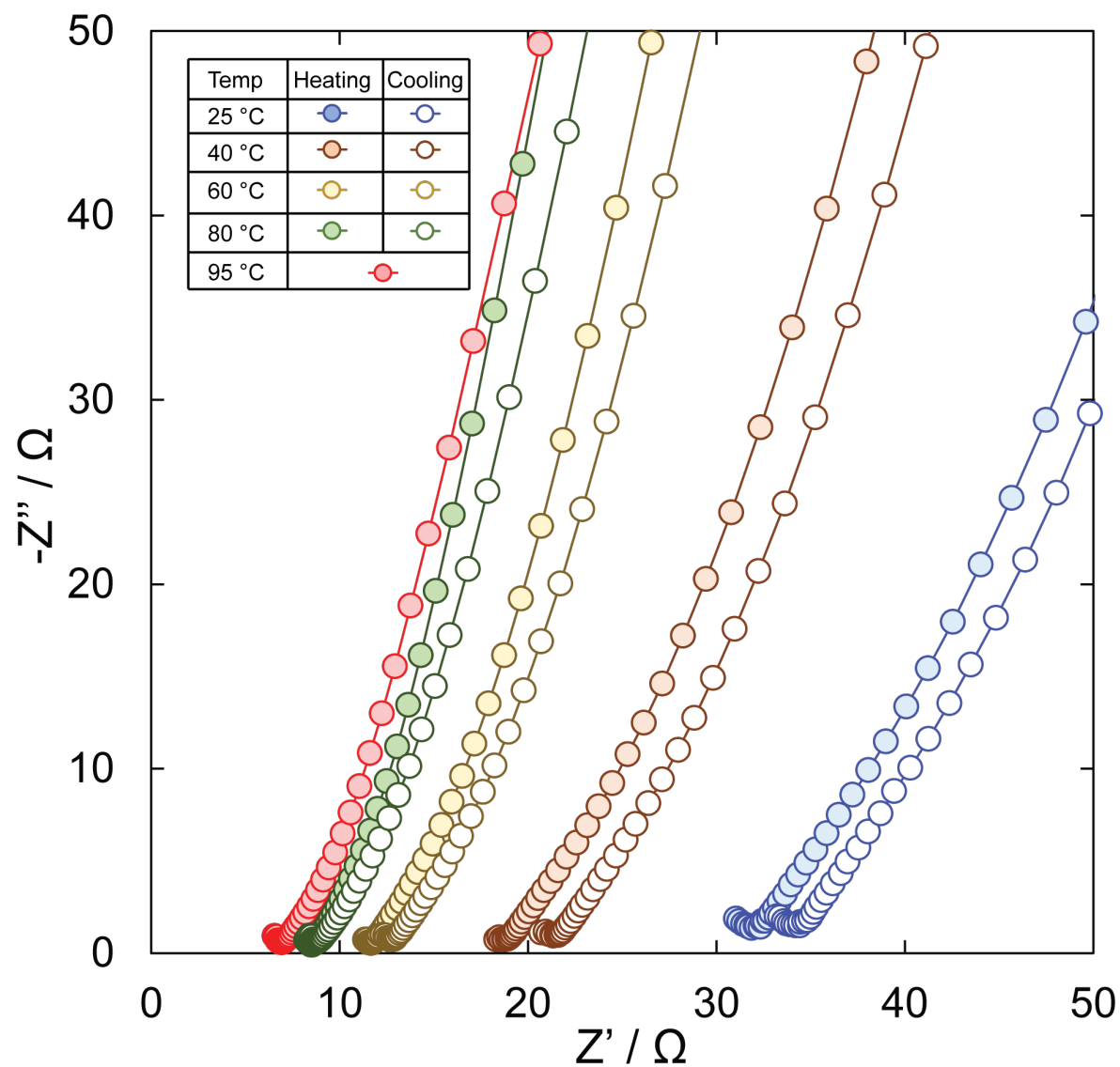


Fig. S13. Nyquist plots resulting from ac impedance analysis of pelletized VNU-15 under 55% RH when heating and cooling from 25 °C to 95 °C.

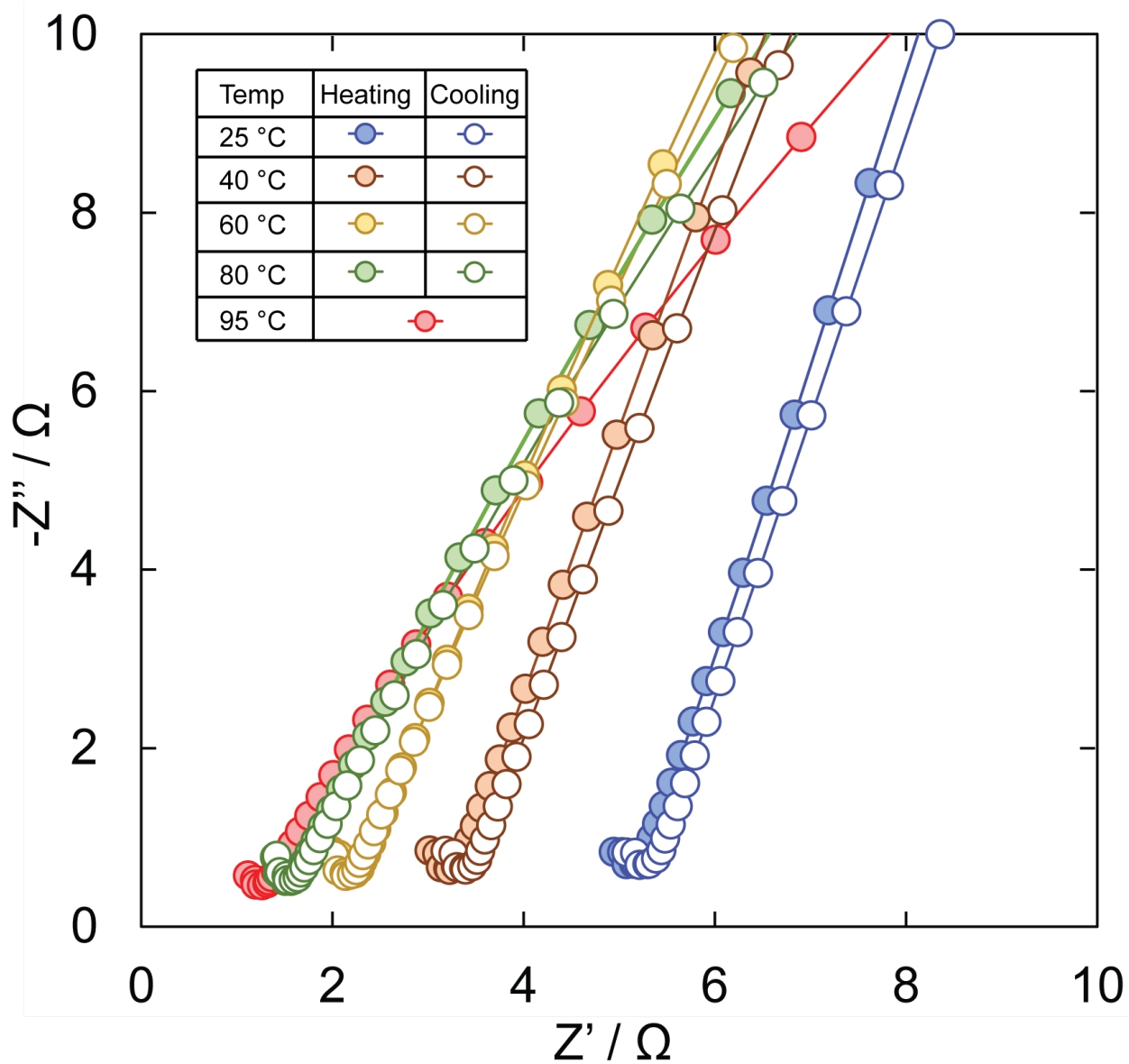


Fig. S14. Nyquist plots resulting from ac impedance analysis of pelletized VNU-15 under 60% RH when heating and cooling from 25 °C to 95 °C.

Table S3. Temperature & proton conductivity dependence of pelletized VNU-15 at 55 and 60% RH.

RH / %	Temp / °C	σ / S cm ⁻¹	
		Heating	Cooling
60	25	0.70×10^{-2}	0.68×10^{-2}
	40	1.1×10^{-2}	1.0×10^{-2}
	60	1.6×10^{-2}	1.6×10^{-2}
	80	2.3×10^{-2}	2.3×10^{-2}
	95	2.9×10^{-2}	
55	25	0.95×10^{-3}	0.91×10^{-3}
	40	1.62×10^{-3}	1.46×10^{-3}
	60	2.70×10^{-3}	2.47×10^{-3}
	80	3.69×10^{-3}	3.53×10^{-3}
	95	4.70×10^{-3}	

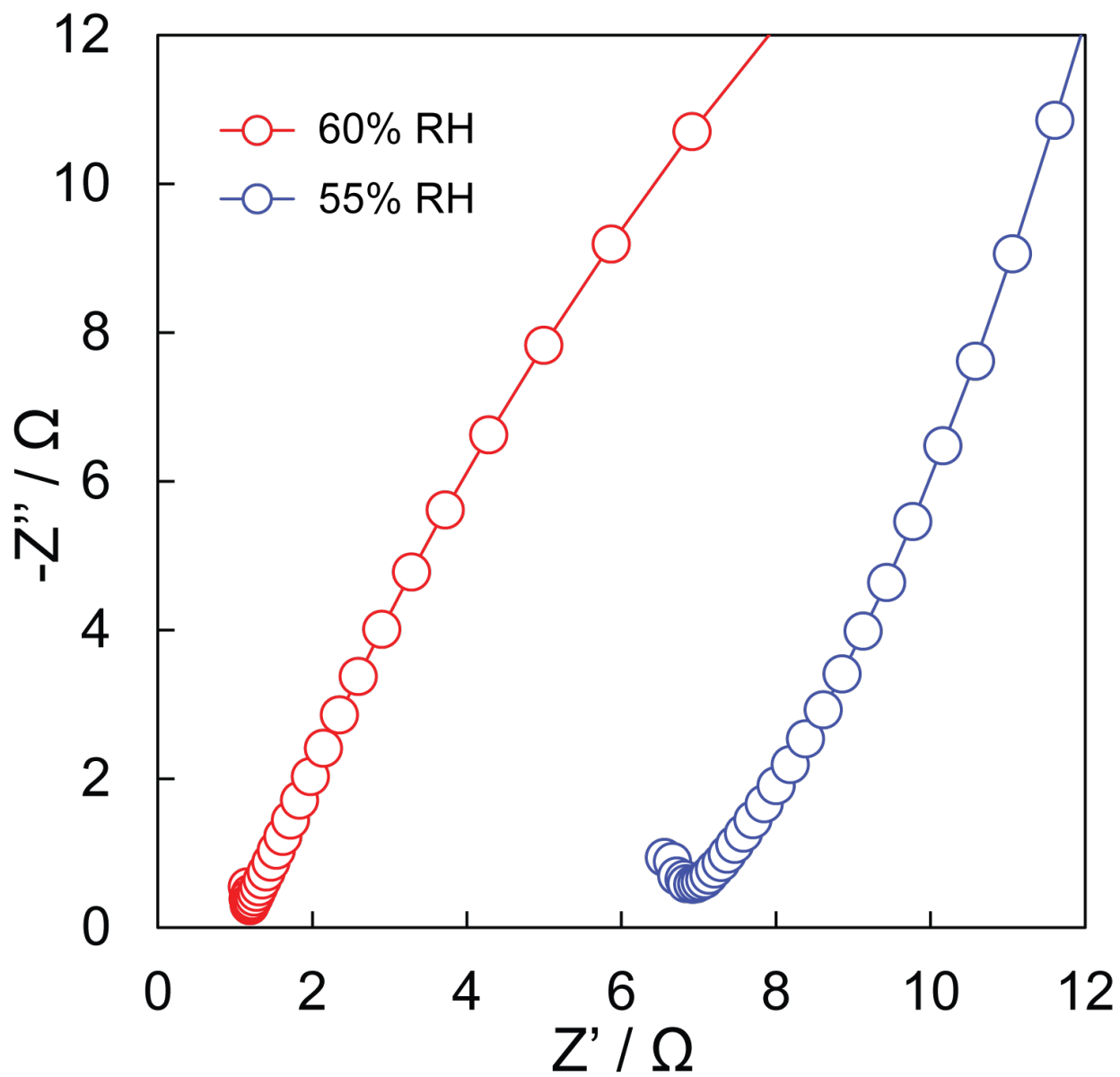


Fig. S15. Nyquist plot of pelletized VNU-15 at 55 (blue circles) and 60% RH (red circles) at 95 °C after 40 h of consecutive ac impedance measurements.

Section S9: Stability of VNU-15 during Proton Conductivity Studies

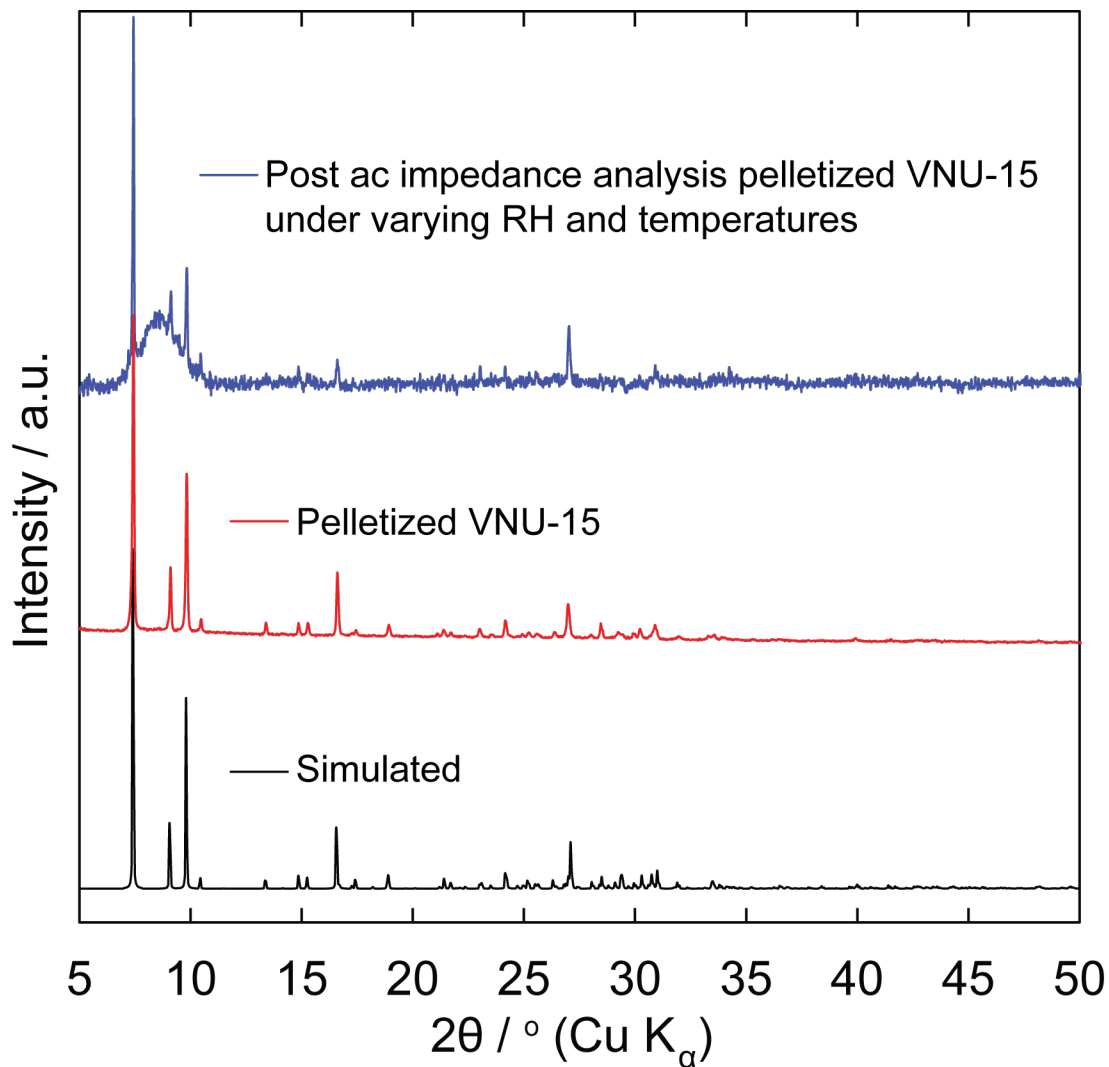


Fig. S16. Simulated PXRD pattern of VNU-15 (black) as compared to the experimental patterns from the pelletized VNU-15 (red) and subjecting pelletized VNU-15 to 30, 40, and 50% RH for 16 h at each RH followed by ac impedance analysis at temperatures ranging from 25 to 95 °C (blue).

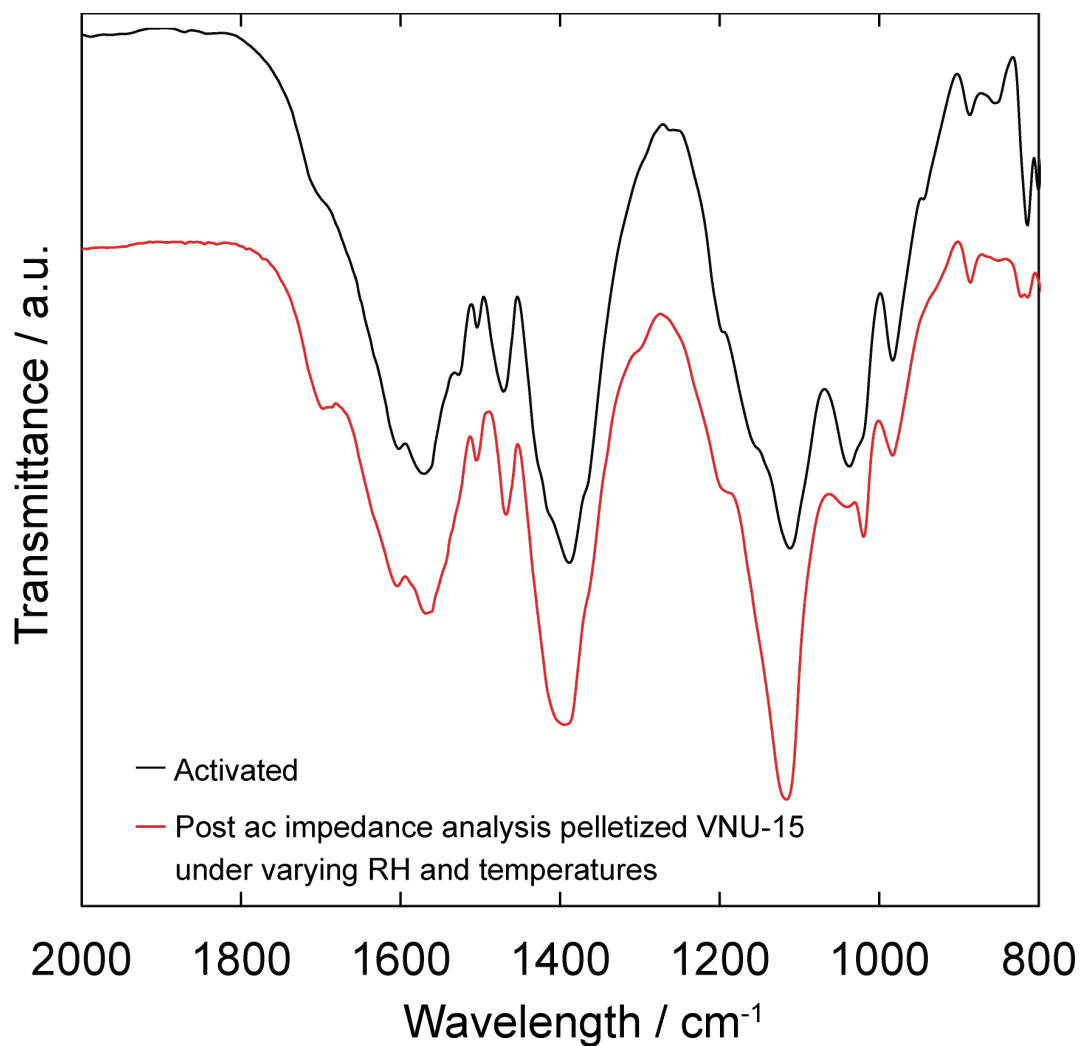


Fig. S17. FT-IR of activated VNU-15 (black) as compared to the experimental spectrum after subjecting pelletized VNU-15 to 30, 40, and 50% RH for 16 h at each RH followed by ac impedance analysis at temperatures ranging from 25 to 95 °C (red).

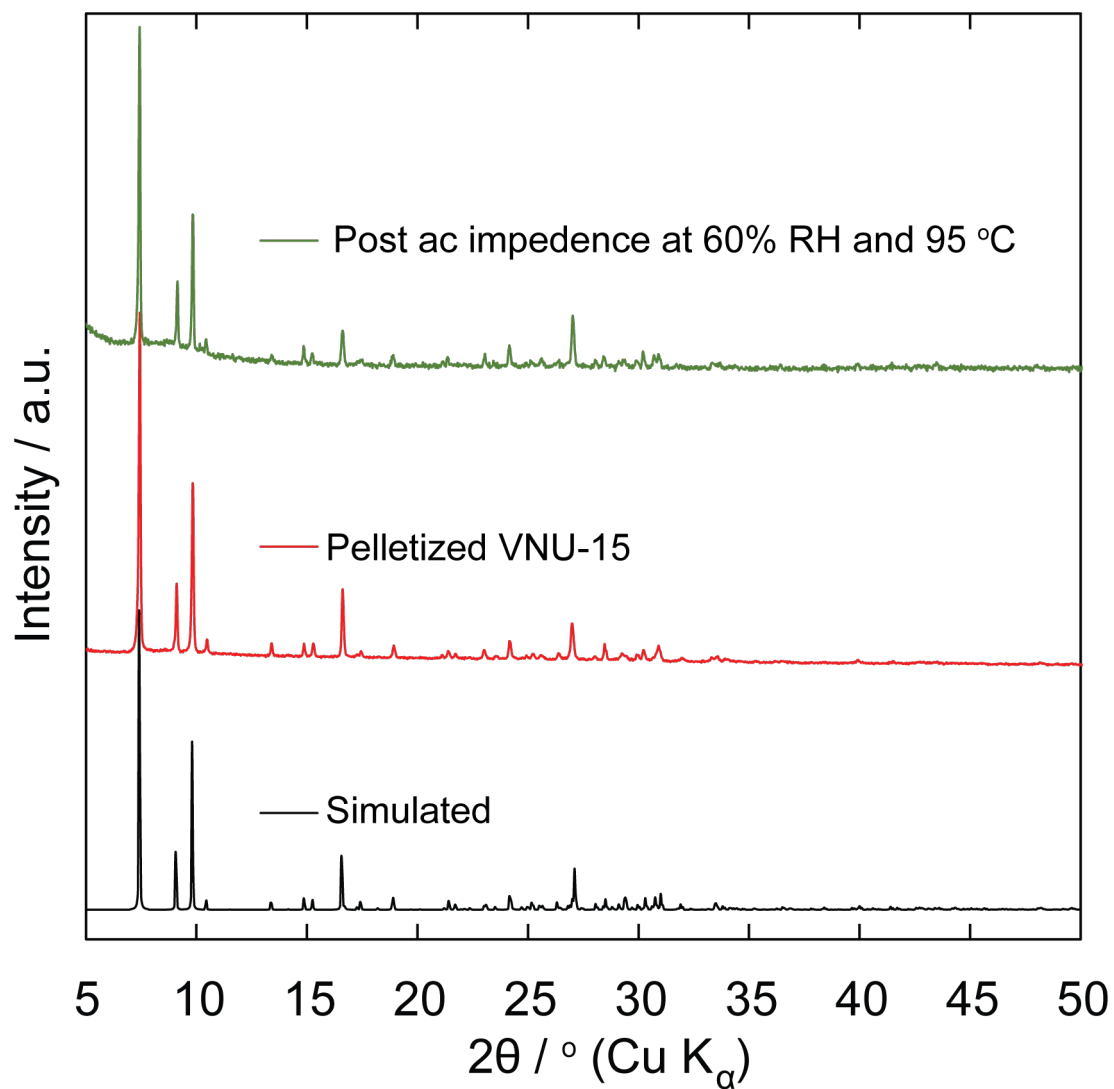


Fig. S18. Simulated PXRD pattern of VNU-15 (black) as compared to the experimental patterns from pelletized VNU-15 (red) and subjected to 60% RH for 16 h followed by ac impedance analysis (green).

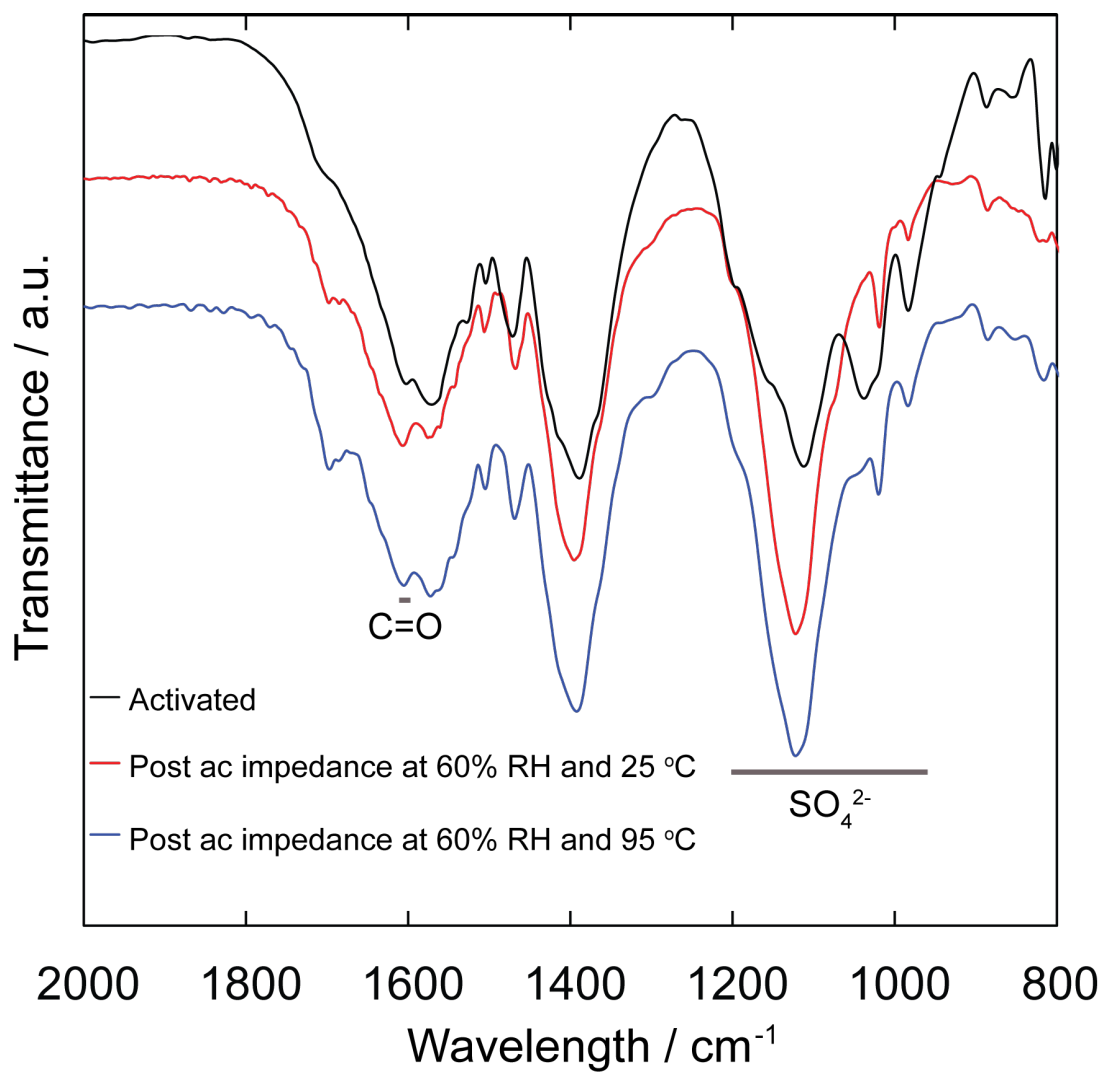


Fig. S19. FT-IR of activated VNU-15 (black) as compared to the experimental spectra of pelletized VNU-15 that was subjected to 60% RH for 16 h followed by ac impedance analysis at 25 °C (red) and 95 °C (blue).

Section S10: References

1. A. L. Spek, *Acta Cryst.*, 2009, **D65**, 148-155.
2. P. Horcajada, C. Serre, G. Maurin, N. A. Ramsahye, F. Balas, M. V. Regí, M. Sebban, F. Taulelle and G. Férey, *J. Am. Chem. Soc.*, 2008, **130**, 6774-6780.
3. S. Surblé, C. Serre, C. M. Draznieks, F. Millange and G. Férey, *Chem. Commun.*, 2005, **3**, 284-286.
4. J. M. Taylor, K. W. Dawson and G. K. Shimizu, *J. Am. Chem. Soc.*, 2013, **135**, 1193-1196.